Identification of heterogeneous elastoplastic behaviors using constitutive equation gap method

Tarik Madani, Yann Monerie, Stéphane Pagano, Céline Pelissou, Bertrand Wattrisse

IDENTIFICATION OF HETEROGENEOUS ELASTOPLASTIC BEHAVIORS USING CONSTITUTIVE EQUATION GAP METHOD – ADMOS 2015

T. MADANI[1, 3], Y. MONERIE[2, 3], S. PAGANO[2, 3], C. PELISSOU[1, 3], B. WATTRISSE[2, 3]

1 Institut de Radioprotection et de Sureté Nucléaire, IRSN/PSN/SEMIA, Bat. 702, BP3-13115 Saint-Paul-lez-Durance Cedex, France
2 Laboratoire de mécanique et génie civil, Université de Montpellier (LMGC), Pl. E. Bataillon, Montpellier, France
3 Le Laboratoire de micromécanique et intégrité des structures (MIST), IRSN-CNRS-Université de Montpellier

{tarik.madani, yann.monerie, stephane.pagano, bertrand.wattrisse}@univ-montp2.fr, celine.pelissou@irsn.fr

Key words: Inverse method, Material identification, Elastoplasticity, Full field measurement.

Abstract. To be able to identify cohesive zone models for heterogeneous materials, we need to estimate the local stress fields. The recent developments in imaging techniques allow now reaching local measurement fields (*e.g.* strain, temperature…). In this paper, an iterative procedure is used to identify the spatial material properties distribution and the local stress fields. The formulation and the principle of the method are presented, and its reliability is checked using finite element simulation data as reference full-field measurements. Finally, the method is applied on noisy measured displacement fields to assess its robustness.

1 INTRODUCTION

Various identification techniques are developed to identify mechanical behaviors and stress fields using kinematic field variables such as displacements or strains obtained by full-field measurements techniques (like Digital Image Correlation (DIC), interferometric techniques, grid methods, etc.). An overview of these identification procedures and their applications on experimental data can be found in [1].

In this work, we extend and adapt the approach developed in [2, 3] to identify the constitutive laws and their mechanical parameters for heterogeneous materials. The class of models that we have in mind is J2-based hardening elastoplasticity. Such identification requires the knowledge of the local stress fields. The Constitutive Equation Gap Method (CEGM) originally used as an error estimator for finite element simulations is here adopted in order to identify these fields in heterogeneous materials.

For the identification of plastic parameters, we introduce the elastoplastic secant stiffness tensor B^s. For a linear kinematic Prager model, the tensor B^s is expressed directly as a function of the material properties (elastic constants: Young modulus E and Poisson ratio ν

for isotropic elasticity and shear modulus G for cubic elasticity, yield stress σ_0 and hardening coefficient k) and of the loading history. In the following, we will present first the identification procedure, then the performance of the method will be illustrated on various examples using simulated data obtained under small perturbations and plane stress assumptions. We will then check its robustness with respect to measurement noise.

2 INVERSE METHOD

2.1 Identification procedure

The procedure is presented in a 2D framework (plane stress) because it will be used on thin, flat samples observed *via* in-plane DIC techniques. Consequently, we focus here on the identification of elastoplastic constitutive laws in a 2D framework. In the context of identification of heterogeneous stress fields, three material parameters can be locally identified at most because we have only access to the three local in-plane strain measurements.

The CEGM is based on the minimization of an energetic functional and depends on two sets of parameters: the stress field and the mechanical material properties. This procedure is applicable to any identification problem and can be used with data extracted from numerical simulations (for validation purposes, as in the present paper) or experimental measurements.

For a sequence of successive load steps (subscript n for each step), we denote the measured displacement field $\vec{u}_n^m$ on a given region of interest Ω of a specimen and we consider an elastoplastic body, governed by the set of equations (1, 2, and 3):

$$div\ \underline{\sigma_n^c} = 0 \quad in\ \partial\Omega \tag{1}$$

$$\underline{\sigma_n^c} = \underline{\underline{B_n^s}} : \underline{\varepsilon}\left(\vec{u}_n^m\right) \quad in\ \partial\Omega \tag{2}$$

$$\begin{cases} \vec{R}_j = \int_{\partial\Omega_j} \underline{\sigma_n^c}\vec{n}\ ds \quad on\ \partial\Omega_j \\ \underline{\sigma_n^c}\vec{n} = 0 \quad on\ \partial\Omega_i \end{cases} \tag{3}$$

where σ_n^c and $\underline{\varepsilon}$ represent the stress and strain tensors, $\underline{\underline{B^s}}$ is the fourth order secant elastoplastic tensor (corresponding to the standard Hooke tensor $\underline{\underline{B^e}}$ for an elastic step). It is important to notice that for a heterogeneous material, all these quantities depend on the position.

The overall forces $\vec{R}_j$ are known on the boundary $\partial\Omega_j$ of Ω .The free boundaries $\partial\Omega_i$ satisfy the relations: $\partial\Omega_j \cup \partial\Omega_i = \partial\Omega$ and $\partial\Omega_j \cap \partial\Omega_i = \emptyset$. In the case of a cubic material, the Hooke tensor $\underline{\underline{B^e}}$ depends only on three elastic constants: E, G, and ν.

The energetic functional can be expressed in its simplest form (small strain hypothesis, equilibrium):

$$E_{rc}\left(\vec{u}_n^c, \underline{\underline{B_n^s}}\right) = \frac{1}{2}\int_1^t \int_\Omega \left[\underline{\varepsilon}\left(\vec{u}_n^c\right) - \underline{\varepsilon}\left(\vec{u}_n^m\right)\right] : \underline{\underline{B_n^s}} : \left[\underline{\varepsilon}\left(\vec{u}_n^c\right) - \underline{\varepsilon}\left(\vec{u}_n^m\right)\right] d\Omega dt \tag{4}$$

where $\vec{u}_n^c$ is a displacement field compatible with equilibrium of the studied domain Ω.

The identification procedure consists in minimizing E_{rc} with respect to $\vec{u}_n^c$ and $\underline{\underline{B_n^s}}$.

According to [4], the fourth order secant elastoplastic tensor can be written at load step n as:

$$\underline{\underline{B_n^s}} = \left[\underline{\underline{B^{e^{-1}}}} + \frac{\Delta\gamma_n}{1+\frac{2}{3}k\Delta\gamma_n}\underline{\underline{P}}\right]^{-1} \tag{5}$$

and with respect to the material parameters:

$$\underline{\underline{B_n^s}} = \begin{bmatrix} \frac{E(1+2KE)}{3K^2E^2-2KE(\nu-2)+1-\nu^2} & \frac{E(\nu+KE)}{3K^2E^2-2KE(\nu-2)+1-\nu^2} & 0 \\ \frac{E(\nu+KE)}{3K^2E^2-2KE(\nu-2)+1-\nu^2} & \frac{E(1+2KE)}{3K^2E^2-2KE(\nu-2)+1-\nu^2} & 0 \\ 0 & 0 & \frac{G}{1+6KG} \end{bmatrix} \tag{6}$$

where $\underline{\underline{P}}$ is a constant mapping matrix:

$$P = \frac{1}{3}\begin{bmatrix} 2 & -1 & 0 \\ -1 & 2 & 0 \\ 0 & 0 & 6 \end{bmatrix}. \tag{7}$$

and $\Delta\gamma_n$ is the plastic multiplier at load step n

$$\Delta\gamma_n(\sigma_0, k) = \frac{3}{2k}\langle\sqrt{\frac{3}{2}}\frac{\underline{\underline{\alpha_n}}}{\underline{\underline{\sigma_0}}} - 1\rangle^+ \tag{8}$$

with $\langle a\rangle^+$ representing the positive part of a, $\underline{\underline{\alpha_n}}$ the second invariant of the effective stress $\left(\underline{\underline{\sigma_n^c}} - \underline{\underline{X_n}}\right)$, X_n is the backstress tensor, reached at the current load step

$$\underline{\underline{\alpha_n}}^2 = \left(\underline{\underline{\sigma_n^c}} - \underline{\underline{X_n}}\right)^T \cdot \underline{\underline{\underline{P}}} \cdot \left(\underline{\underline{\sigma_n^c}} - \underline{\underline{X_n}}\right). \tag{9}$$

And finally, as we know that $\underline{\underline{\varepsilon_p}} = \underline{\underline{\varepsilon_e}} - \underline{\underline{\underline{B}}}^{e^{-1}} : \underline{\underline{\sigma_c}}$ we can write K, depending on two parameters (function of σ_0 and k):

$$K = a\frac{\|\varepsilon^p\|}{b + \|\varepsilon^p\|} \tag{10}$$

2.2 Numerical method

We focus on a J2 elastoplastic model with kinematic hardening. The elastic and plastic identification problem consists in finding the elastoplastic secant stiffness tensor $\underline{\underline{\underline{B_n^s}}}$ and the stress field satisfying equations (1) to (3). Thanks to the convexity of the cost-function E_{rc}, the minimization can thus be performed in two consecutive steps: first with respect to the displacement field $\vec{u}_n^c$ associated with a statically admissible stress fields $\underline{\underline{\sigma_n^c}}$ and second with respect to the secant tensor $\underline{\underline{\underline{B_n^s}}}$ to identify the material parameters. These steps are presented in the figure 1.b and this algorithm is used to compute the elastic and plastic properties.

The identification algorithm involves three steps: (*i*) an elastic identification, (*ii*) a plasticity detection and (*iii*) a plastic identification. The Steps (*i*) and (*iii*) are based on the minimization of the E_{rc} cost function. This minimization is performed through an iterative algorithm illustrated in Figure 1.b (example for an elastic identification), starting from an initial set of parameters ($\underline{\underline{\underline{B_0}}}$). The procedure is stopped using a convergence criterion on the norm of the tangent tensor. At convergence, the CEGM procedure gives the material parameters and the stress field.

The elastic identification (step (*i*)), involves an analytic minimization of E_{rc} with respect to the material parameters (E, ν, G) [2]. The plastic identification is less direct since the secant tensor expression requires the knowledge of the stress state. The plastic step is initialized with the result of an elastic identification. Naturally, the elastic constants obtained

by this identification are not the desired parameters, but they give a first estimation of the secant tensor at the current loading step $\underline{\underline{B_0^s}}$, and a statically admissible stress state. The second step of the minimization then consists in minimizing E_{rc} with respect to parameters a and b. Once the procedure has converged, we get the stress field $\underline{\sigma_n^c}$ and the optimal values (a_{opt}, b_{opt}) that are directly related to the material parameters σ_0 and k.

The plasticity detection (step (*ii*)) consists in comparing the norm of the difference between the identified secant tensor $(\underline{\underline{B_n^s}})_i$ at iteration i and the one identified at the previous (i-1) iteration: $(\underline{\underline{B_n^s}})_{i-1}$ with the norm of $(\underline{\underline{B_n^s}})_{i-1}$:

$$\left\| (\underline{\underline{B_n^s}})_i - (\underline{\underline{B_n^s}})_{i-1} \right\|_2 < \epsilon \left\| (\underline{\underline{B_n^s}})_i \right\|_2 \tag{11}$$

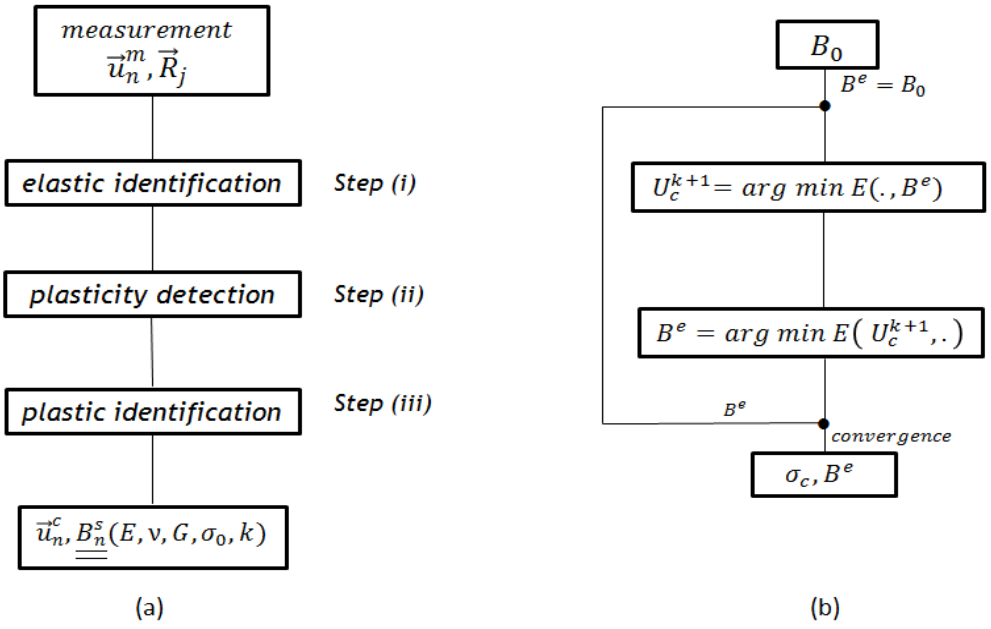

Figure 1- (a) Elastoplastic algorithm, (b) Example of E_{rc} minimization elastic algorithm used for the step(i) and step(iii).

For the first loading steps, and as long as no plasticity occurs, the secant tensor is equal to the elastic tensor $\underline{\underline{B^e}}$.

3 VALIDATIONS

In this section, the efficiency of the proposed procedure is examined using reference simulated measurements obtained with the finite element code Comsol Multiphysics. No experimental data are presently processed. Only simulated measurements are considered to focus on the identification procedure. The in-plane components of the displacement field are extracted at the nodes of the finite element discretization and the global load levels are extracted on the outer boundaries. The identification method is tested on numerical examples concerning both homogeneous and heterogeneous materials subjected to a tensile test. Moreover, the robustness of the method is illustrated by studying its sensitivity on noisy data.

3.1 Results

a. Elastic identification

The first (specimen 1) test is performed on an elastic bi-material sample: a soft circular isotropic inclusion (Young modulus of 100 GPa, Poisson ratio of 0.15) is embedded in a stiff isotropic matrix (Young modulus 210 GPa, Poisson ratio 0.3). Two types of identification are performed:

- an identification mesh perfectly consistent with the material domains (two identification domains D_1 inclusion and D_2 matrix);
- An identification mesh that does not match the material heterogeneity by decomposing it into 400 domains D_j with j = 1 to 400.

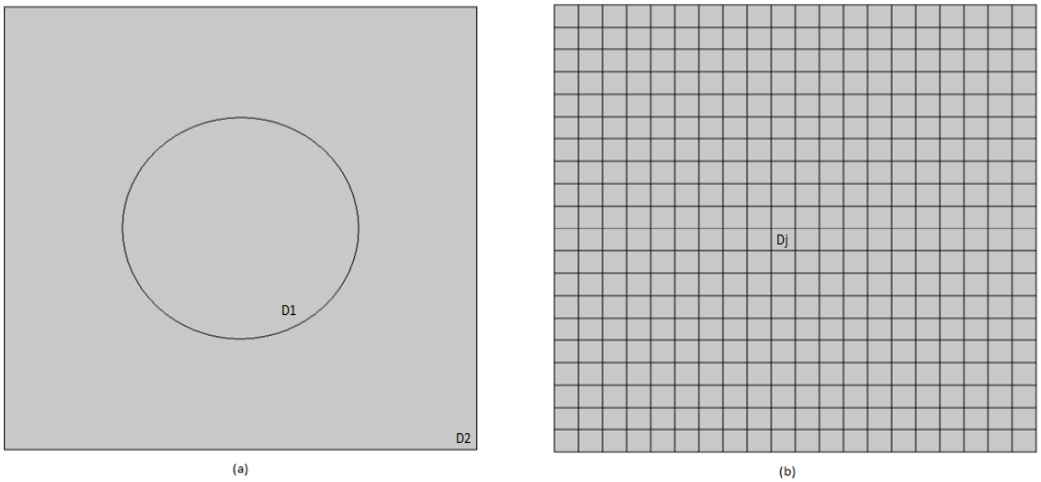

Figure 2- Geometry for the identification: (a) two identification domains respecting the material heterogeneity and (b) 400 identification domains that do not respect the material heterogeneity.

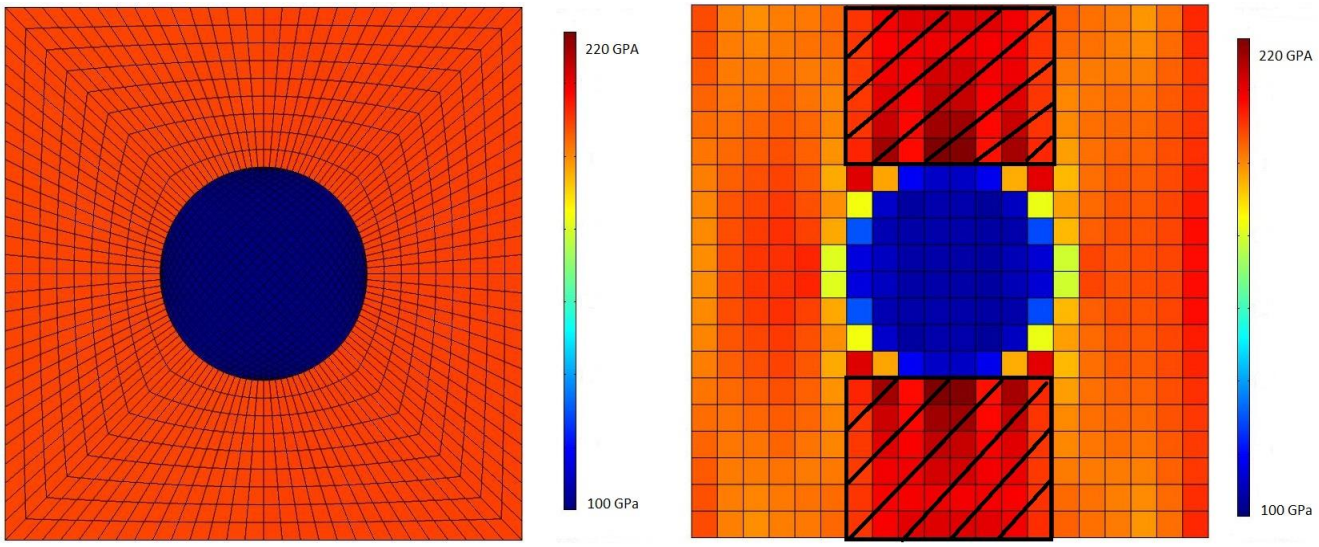

(a) (b)

Figure 3- Identified Young modulus distributions: (a) 2 « consistent » identification domains and (b) 400 « inconsistent » identification domains.

For the first identification, the figure 3 shows a good prediction of the parameter sets with a relative error about 1%. Moreover only one load level is sufficient to identify those parameters. So the computational time of the procedure is very fast. The Figure 4 shows that the identified stress fields are very close to the reference values.

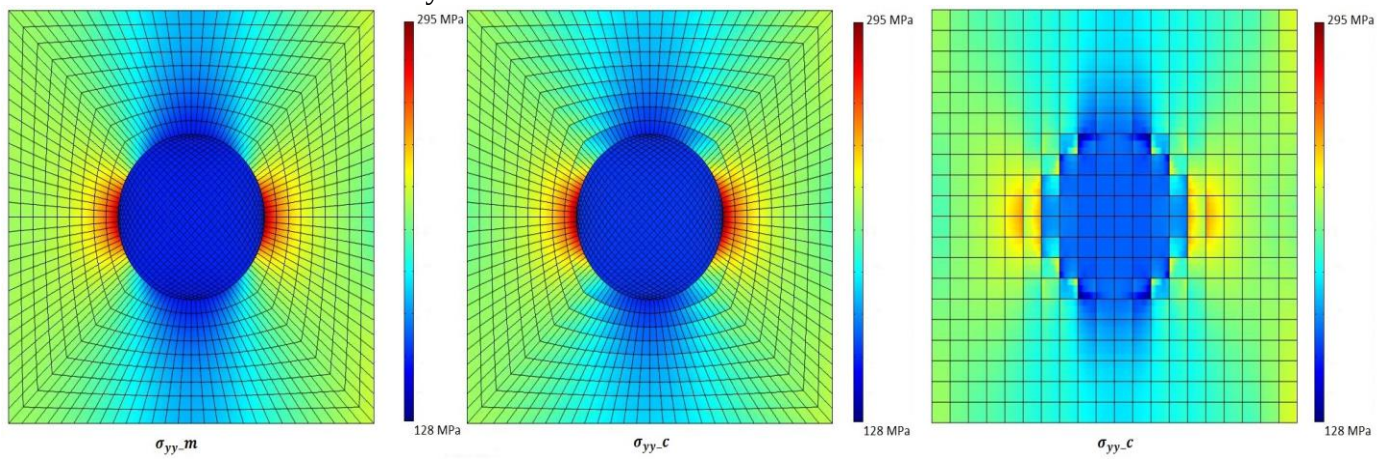

(a) (b) (c)

Figure 4- Distribution of transversal stress fields: (a) "measured" stress field $\sigma_{yy\_}m$ (from FE simulation), (b) identified stress field $\sigma_{yy\_}c$ using 2 "consistent" identification domains and (c)identified stress field $\sigma_{yy\_}c$ using 400 "inconsistent" identification domains.

For the second identification (400 "inconsistent" material domains), the inclusion is perfectly localized. This result shows the ability of the technique to identify heterogeneous elastic properties but the identification technique is based on a minimization of an energy norm formulated upon the CEGM and if this energy is very small the local identification cannot be performed (zones located above and under the inclusion). Furthermore, the error is greater in the domains where the strain gradients are high. The presence of strain gradients is

an important source of identification errors. The computational time is more important because we identify 800 parameters instead of 4 but the results are consistent and show the feasibility of this approach.

b. Elastoplastic identification

The second test (specimen 2) concerns a standard tensile test performed at constant velocity on an isotropic elastoplastic material (Young modulus 210 GPa, Poisson ratio 0.3, yield stress σ_0 300 MPa and hardening modulus k 1 GPa). The material parameters are identified using data associated with 5 load steps (2 in the elastic domain, and 3 in the plastic domain). Although the material is homogeneous, the identification is made on 4 material domains (figure 6).

Identified parameters obtained from each zone are collected in the table 1. As it can be noticed, the identified parameters values are very close to the reference values and are very similar from one identification domain to another.
The reference ("measured") stress fields presented in figure 6.a are obtained by solving the direct problem whereas the stress fields presented in figure 6.b are obtained by the inverse method. We note a close similarity between the distributions and the orders of magnitude for this stress component. The procedure converges in a few iterations. The identification of the parameters and stress fields gives very satisfactory results (see Table 1).

Table 1: Identifed parameters: specimen 2.

Parameters	E (GPa)	ν	k (GPa)	σ_0 (MPa)
Reference values	210,00	0,30	1,00	300,00
Z1	209.80	0,30	1,03	298,49
Relative difference (%)	0,10	0,00	3,00	0,50
Z2	210,05	0,30	0,99	299,51
Relative difference (%)	0,02	0,00	1,00	0,16
Z3	210,12	0,30	1,00	299,38
Relative difference (%)	0,06	0,00	0,00	0,21
Z4	209,86	0,30	0,99	299,60
Relative difference (%)	0,07	0,00	1,00	0,13

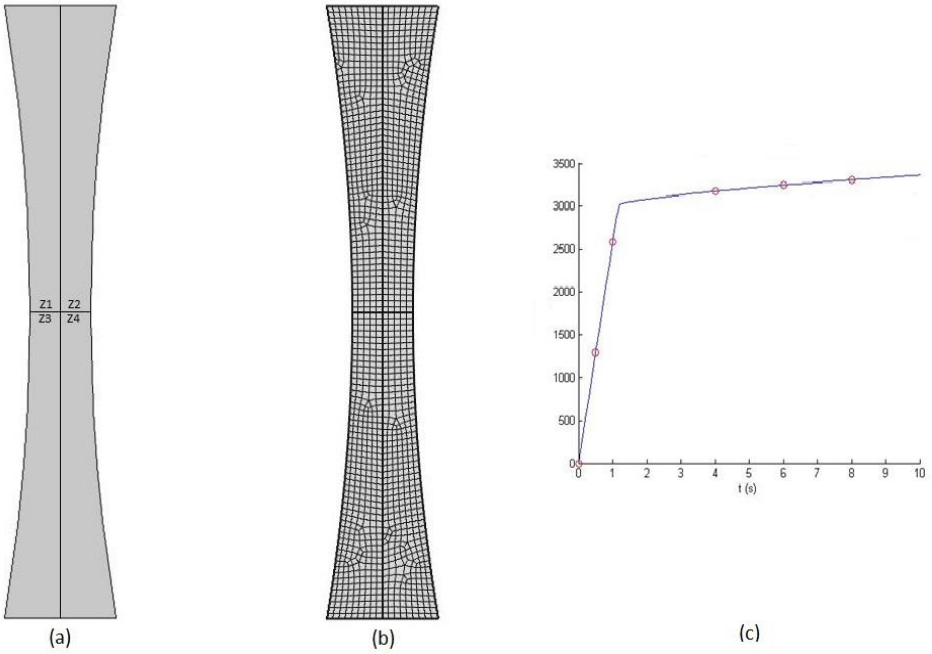

Figure 5- (a) Geometry and identification domains, (b) identification mesh (1400 elements) and (c) the 5 load steps.

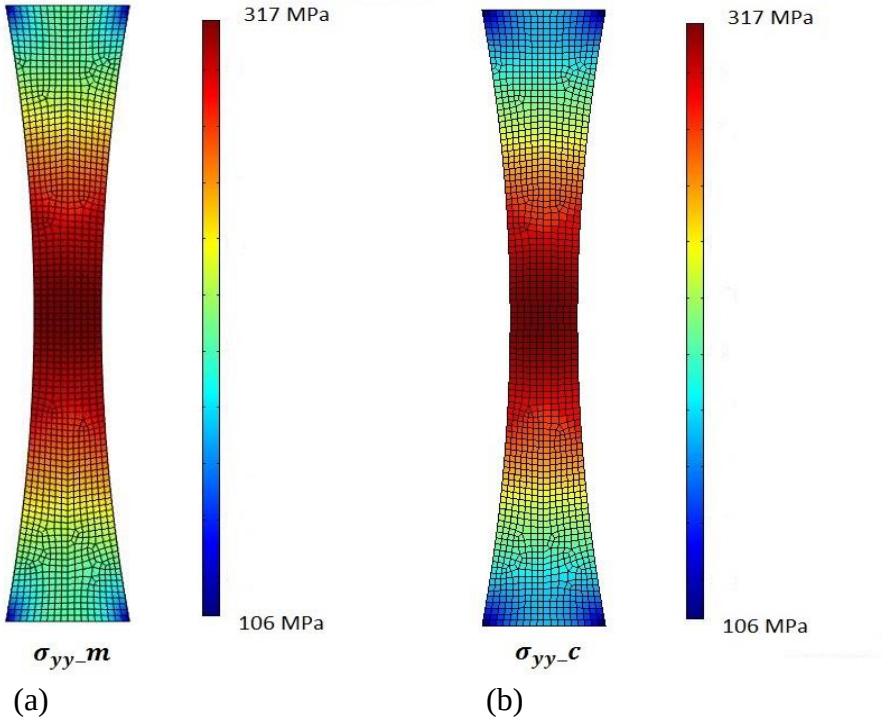

Figure 6- Distribution of transversal stress fields: $\sigma_{yy\_}m$ from FE simulation and $\sigma_{yy\_}c$ the identified.

3.2 Sensitivity to the initial set of parameters

To assess the sensitivity of the identification results to initial values, different starting values of the parameters are selected for the procedure. The identification is performed on the specimen 2 (table 1) and we check the number of iteration needed for the convergence of the procedure.

Table 2 shows that the obtained parameters are in good agreement whatever the chosen initial value. So, we can see the stability of the identification procedure of the influence of the initial parameters. This confirms the uniqueness of the solution and the independence of the solution to the initial values.

Table 2: Sensitivity to initial set of parameters : specimen 2.

Parameters	E (GPa)	ν	k (GPa)	σ_0(MPa)
Reference values	210	0,3	1	300
Initial value 1	1,00E-09	1,00E-09	1,00E-09	1,00E-09
Identified values	209,74	0,30	1,03	300,10
Relative difference (%)	0,12	0,00	3,00	0,03
Number of iteration	7	7	8	8
Initial value 2	155,00	0,15	0,50	150,00
Identified values	209,77	0,30	1,03	300,10
Relative difference (%)	0,11	0,00	3,00	0,03
Number of iteration	7	7	6	6
Initial value 3	420,00	0,60	2,00	600,00
Identified values	209,84	0,30	1,03	300,09
Relative difference (%)	0,08	0,00	3,00	0,03
Number of iteration	8	8	6	6

3.3 Sensitivity to mesh refinement

In this paragraph we will see also the efficiency of the identification with mesh refinement. We mesh the specimen 2 with three different element sizes (coarse, normal and fine meshes) to check the convergence of the procedure.

Table 3: Sensitivity to mesh density : specimen 2.

Parameters	E (GPa)	ν	k (GPa)	σ_0(MPa)
Reference values	210,00	0,30	1,00	300,00
Coarse mesh				
Identified values	209.80	0,30	1,03	300,09
Relative difference (%)	0,10	0,00	3,00	0,03
Normal mesh				
Identified values	209,94	0,30	0,99	302,79
Relative difference (%)	0,03	0,00	1,00	0,93
Fine mesh				
Identified values	209,94	0,30	1,00	299,63
Relative difference (%)	0,03	0,00	0,00	0,12

The identification is performed for each mesh, and the results obtained on specimen 2 are reported in Table 3. As it can be noticed, the identified parameters values are very similar.

3.4 Sensitivity to experimental noise

The robustness of the CEGM approach with respect to noise is evaluated using a set of simulated displacement fields disturbed by a white noise at different levels. For this purpose, we perform an identification on an homogeneous isotropic material submitted to a tensile test. The noise level is chosen $\boldsymbol{\gamma = 0.01\ pixel}$. This value is consistent with typical DIC measurement errors. The reference FE-displacement fields are corrupted by a white Gaussian noise with the amplitude $\boldsymbol{\gamma}$.

Table 3: Sensitivity to noise : specimen 2.

Parameters	E (GPa)	ν	k (GPa)	σ_0 (MPa)
Reference values	210	0,3	1	300
Random noise amplitude **0.1*γ**				
Identified values	209,79	0,30	0,99	300,17
Relative difference (%)	0,10	0,00	1,00	0,06
Random noise amplitude **γ**				
Identified values	206,96	0,30	0,99	299,84
Relative difference (%)	1,45	0,00	1,00	0,05

Random noise amplitude **2*γ**				
Identified values	189,56	0,23	0,96	300,46
Relative difference (%)	11,16	23,33	4,00	0,15

It can be seen that identification of all parameters is stable in presence of noise. Naturally, the elastic constants are more corrupted by the noise level because for a fixed noise level, the signal to noise ratio is smaller for the elastic identification than for the plastic one. Furthermore, the Poisson ratio is more sensitive to noise.

4 CONCLUSIONS

In the present work, we use full-field measurements and the constitutive equation gap method to identify the spatial distribution of a set of J2 elastoplastic behaviors. It is possible to identify the unknown parameters zone by zone, thus allowing to characterize heterogeneous materials. We validate this approach on different situations (heterogeneous elastic materials using heterogeneous strain fields, homogeneous plastic material using heterogeneous strain fields and homogeneous plastic materials using homogeneous strain fields). The identification algorithm has been presented. Numerical simulations show the feasibility and the robustness of the method. The errors in the identification increase in the presence of strong gradients and with the level of measurement noise. The next step will focus on the application of this method to real full-field measurements.

REFERENCES

[1] S. Avril, M. Bonnet, A.S. Bretelle, M. Grediac, F. Hild, P. Ienny, F. Latourte, D. Lemosse, S. Pagano, E. Pagnacco. *Overview of identification methods of mechanical parameters based on full-field measurements*. Experimental Mechanics 48, 381-402, (2008).

[2] F. Latourte, A. Chrysochoos, S. Pagano and B. Wattrisse. *Elastoplastic behavior identification for heterogeneous loadings and materials*. Experimental Mechanics 48 435-449, (2008).

[3] S. Wen, Y. Monerie, B. Wattrisse. *Identification of cohesive zone models from thermomechanical imaging techniques*, CFRAC 2013, (2013).

[4] V. Richefeu A. Chrysochoos, V. Huon, Y. Monerie, R. Peyroux and B. Wattrisse. *Towards local identification of cohesive zone models using digital image correlation*, European Journal of Mechanics - *A/Solids* 34 38-51, (2012).

[5] JC. Simo and TJR. Hughes. *Computational inelasticity*. Springer, pp 126–130, (1998).